



Insights into the degradation of microplastics by Fenton oxidation: From surface modification to mineralization

David Ortiz^{a,*}, Macarena Munoz^{a,**}, Julia Nieto-Sandoval^a, Cristina Romera-Castillo^b, Zahara M. de Pedro^a, Jose A. Casas^a

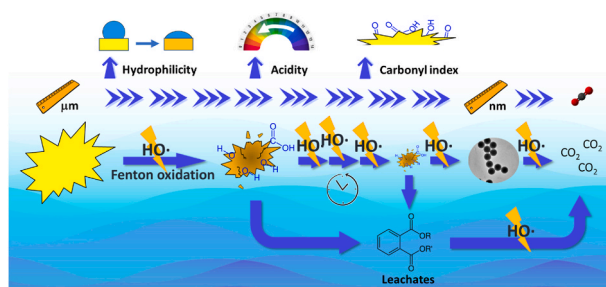
^a Chemical Engineering Department, Universidad Autonoma de Madrid, Ctra. Colmenar Km 15, 28049, Madrid, Spain

^b Instituto de Ciencias del Mar-CSIC, Paseo Marítimo de la Barceloneta, 37, 08003, Barcelona, Spain

HIGHLIGHTS

- Oxidation reaction proceeds from the surface to the core of plastic particles.
- MPs suffered physical alterations and chemical changes along Fenton oxidation.
- MPs decreased their size upon oxidation, eventually leading to their mineralization.
- MPs bearing aromatic rings showed higher oxidation yields than the alkane-based MPs.
- Dissolved leachates generated along the treatment did not inhibit bacterial growth.

GRAPHICAL ABSTRACT



ARTICLE INFO

Handling Editor: Michael Bank

Keywords:

Fenton oxidation
Microplastic
Nanoplastic
Polystyrene

ABSTRACT

This work aims at evaluating the fate of microplastics (MPs) along Fenton oxidation. For such goal, realistic MPs (150–250 μm) of five representative polymer types (PET, PE, PVC, PP and EPS) were obtained from commercial plastic products by cryogenic milling. Experiments (7.5 h) were performed under relatively severe operating conditions: $T = 80\text{ }^{\circ}\text{C}$; $\text{pH}_0 = 3$; $[\text{H}_2\text{O}_2]_0 = 1000\text{ mgL}^{-1}$ (15 doses, 1 every 0.5 h); $[\text{Fe}^{3+}]_0 = 10\text{ mgL}^{-1}$ (5 doses, 1 every 1.5 h). Slight MPs weight losses ($\sim 10\%$) were achieved after Fenton oxidation regardless the MP nature. Nevertheless, oxidation yield clearly increased with decreasing the particle size given their higher exposed surface area (up to 20% weight loss with 20–50 μm EPS MPs). Clearly, MPs suffered important changes in their surface due to the introduction of oxygenated groups, which made them more acidic and hydrophilic. Furthermore, MPs progressively reduced their size. In fact, they can be completely oxidized to CO_2 , as demonstrated in the oxidation of PS nanoplastics (140 nm), where 70% mineralization was achieved. The nature of the plastic particles had a relevant impact on its overall oxidation, being more prone to be oxidized those polymers which contain aromatic rings in their structures (EPS and PET) compared to those formed by alkane chains (PE, PP and PVC). In the latter, the presence of substituents also reduced their oxidation potential. Remarkably, possible leachates released along reaction were more quickly oxidized than the MPs/NPs, so it can be assumed that these dissolved compounds would be completely removed once the solid particles are eliminated. Notably, the leachates obtained upon MPs oxidation were more biodegradable than the released from the fresh solids. All

* Corresponding author.

** Corresponding author.

E-mail addresses: david.ortiz@uam.es (D. Ortiz), macarena.munoz@uam.es (M. Munoz).

this knowledge is crucial for the understanding of MPs oxidation by the Fenton process and opens the door for the design and optimization of this technology either for water treatment or for analytical purposes (MPs isolation).

1. Introduction

Due to their outstanding properties, *i.e.* high chemical and biological resistance, easy moulding and low cost, plastics have become an indispensable material for the industry and modern society. Their annual worldwide production has increased exponentially since the production of the first synthetic polymers in 1950, and it is expected to double in the next 20 years (MacArthur et al. (2016)). In 2020, almost 370 million tonnes of plastic materials are currently produced worldwide (Plastics Europe (2021)).

Despite its benefits to the economy and daily life are undeniable, the generation and mismanagement of plastic waste represents a critical environmental challenge. The so-called microplastics (MPs) and nanoplastics (NPs), plastic debris smaller than 5 mm and 1 μm , respectively (Yang et al. (2021)), are the most widespread plastic residues in the environment. MPs and NPs have been detected in almost all ecosystems, whether in continental and oceanic waters, sediments, soils or even bottled water (Rezania et al. (2018); Cox et al. (2019)). Once in the environment, these plastic debris are ingested by a wide range of organisms, especially the aquatic ones, throughout the different trophic levels, resulting in their introduction into the food chain and the final consumption of MPs and NPs by humans (Enfrin et al. (2020)). Although their effects on human health are not yet well understood, they represent a health risk not only due to their accumulation throughout the body, but also due to their capacity to adsorb other persistent pollutants such as pesticides, heavy metals or pharmaceuticals given their high exposed surface areas (Munoz et al. (2021); Wu et al. (2016)).

In the last few years, the focus has been placed on the possible role of wastewater treatment plants (WWTPs) in the emission of MPs into the environment. Although WWTPs can usually remove up to 95% of the MPs from water, total removal is hardly found (Sol et al. (2020)), so that WWTPs represent one of the dominant sources of MPs into natural waters (Li et al. (2018)). For instance, it has been revealed that 13 billion MPs are released from WWTPs per day in the United States (Mason et al. (2016)), while in Europe, one of the largest WWTPs in Italy, capable of treating water for 1.2 million equivalent population, releases about 160 million MPs per day (Magni et al. (2019)).

Advanced oxidation processes (AOPs) have emerged as promising wastewater treatment technologies for the removal of a wide range of pollutants of emerging concern such as pharmaceuticals, personal care products or pesticides (Magni et al. (2019); Ma et al. (2019); Bhat and Gogate (2021); Serrano et al. (2020)). However, their application for the removal of MPs and NPs has been scarcely investigated. The few publications found in the literature are mainly related to the application of photocatalysis (Ebrahimbabaie et al. (2022); Nabi et al. (2021)). In these studies, generally focused on the design of new photodegradable polymeric materials, slight weight losses and subtle surface modifications of MPs have been reported. Recently, Ariza-Tarazona et al. (2020) proposed a photocatalytic process to remove MPs from water, achieving a weight loss close to 72% for high density polyethylene (HDPE) working at acidic pH and 0 $^{\circ}\text{C}$ but requiring a high catalyst concentration (4 g L^{-1}) and long reaction time (50 h) under visible light.

Fenton oxidation is a particularly attractive AOP due to its high cost-effectiveness ratio. So far, this process has been mainly investigated as a pre-treatment method to isolate MPs from different kinds of waters for analytical purposes (Tagg et al. (2016); Hurley et al. (2018)). In a recent article (Liu et al. (2019)), Fenton oxidation has been employed as an accelerated ageing method for two of the most widespread MPs in watercourses: polystyrene (PS) and polyethylene (PE). Subtle modifications in MPs have been reported during this treatment, such as small weight losses or reduction of mean particle size, but a big knowledge gap seems

to linger on the actual changes and degradation that MPs/NPs may undergo upon Fenton oxidation. It is crucial to analyse all the modifications these persistent particles can suffer along the oxidation process considering their morphology, particle size, hydrophilicity/hydrophobicity and acid/base properties until they are completely oxidized to CO_2 .

This work aims to address this challenging issue by deeply evaluating the fate of MPs along Fenton oxidation. To enhance the extension of the oxidation process, the study was carried out under relatively severe operating conditions (80 $^{\circ}\text{C}$) given the high persistence of plastics. The role of the MPs nature was investigated by using polyethylene terephthalate (PET), polyethylene (PE), polyvinyl chloride (PVC), polypropylene (PP) and expanded polystyrene (EPS) as target pollutants. All of them were obtained from conventional commercial plastic products by cryogenic milling. The impact of the MPs size was afterwards investigated with EPS particles in the range of <50–500 μm . Apart from considering weight losses along the oxidation reaction, MPs were fully characterized to evaluate any significant change on their surface as well as on their size and morphology. Once confirmed that the oxidation of MPs progressively reduced their size and increased their hydrophilicity, the treatment of PS NPs was also investigated to evaluate if the solid particles could be finally mineralized. In the same line, the oxidation of a common plasticizer (diethyl phthalate) as representative leachate compound from MPs/NPs, was also investigated. Finally, the biodegradability of the dissolved compounds leached along MPs oxidation process was also analysed.

2. Materials and methods

2.1. Materials and chemicals

Nitric acid (65%) (CAS No.: 7697-37-2), hydrogen peroxide solution (30% wt.) (CAS No.: 7722-84-1) and diethyl phthalate (99,5%) (CAS No.: 84-66-2) were supplied by Sigma-Aldrich. Iron (III) nitrate nonahydrate (98%) (CAS No.: 7782-61-8) was provided by Panreac. All these compounds were used as received without further purification. Deionized water was used to perform all the experiments.

Commercial plastic products (disposable water bottles, micropipette tips, containers, food trays and pipelines) of different polymer classes (*i.e.* PET, PE, PVC, PP and EPS) were used to obtain the MPs tested in this work (Table 1). A commercial NP sample of monodisperse PS (PS-R-KM248) was purchased from microParticles GmbH to further analyse the effect of the particle size on the Fenton process in the nano size range.

2.2. Microplastics obtention and characterization

MPs were obtained by cutting up the above-mentioned plastic products with stainless-steel scissors. The resulting particles were further grinded using a cryogenic mill (CryoMill, Retsch). The milling cycles had a duration of 2 min at a frequency of 30 Hz. Between them, an intermediate cooling time of 1 min at 5 Hz was applied. The number of cycles was varied depending on the type of plastic grinded. EPS and PP required 2 and 5 milling cycles, respectively, while PET, PE and PVC required 3 milling cycles. The resulting particles were further sieved to obtain MPs of a standard size range of 150–250 μm . To evaluate the effect of MP size on the oxidation yield, EPS was grinded to obtain different size ranges (<50, 50–100, 100–150, 150–250 and 250–500 μm).

Scanning electron microscopy (SEM) and light microscopic images of the MPs were obtained using a JEOL JSM 6335 F and an Eclipse Ci-S/Ci-

L (Nikon) microscopes, respectively. Transmission electron microscopy (TEM) images of the NPs were obtained using a JEOL JEM 2100 microscope. Particle size distribution of MPs was also measured by laser diffraction particle-size analysis using the Mastersizer 3000 (Malvern) equipment. Prior analysis, samples were suspended in a 5% wt. ethylene-glycol aqueous solution. Elemental analyses (CHNS) were performed in a CHNS-932 elemental analyser (LECO Corporation). Water contact angle measurements were carried out in the sessile mode at room temperature (23 °C) using a Dataphysics OCA 15 system. MPs were placed onto a glass sample holder. The sample was manually pressed using a spatula to reach a flat surface, where a drop of water (10 µL) was finally deposited. The determination of the pH_{slurry} of MPs was performed placing 0.2 g of the solid in 10 mL deionized water at different initial pH values (pH₀ = 4, pH₀ = 6, pH₀ = 8). The suspensions were kept in a continuously stirred bottle at room temperature until pH of the slurry was stable (at least, 24 h). Specific surface area of MPs was measured from nitrogen adsorption-desorption isotherms at −196 °C using a Micromeritics Tristar 3020 apparatus. Nevertheless, negligible area values were obtained (<1 m² g^{−1}) in all cases mainly due to the non-porous character of these solids.

To further evaluate the surface chemistry of the plastic particles, Fourier transform infrared spectroscopy (FTIR) spectra of both fresh and oxidized MPs were recorded using a FTIR Bruker IFS66v spectrometer. Analyses were carried out by the attenuated total reflectance (ATR) method using a diamond crystal. The carbonyl index (CI) of the materials was estimated following the procedure described elsewhere (Miranda et al. (2021)). Briefly, CI was calculated as the ratio of the carbonyl peak (1850–1650 cm^{−1}) relative to a reference peak following Eq. (1):

$$CI = \frac{A_{\text{Carbonyl group}}}{A_{\text{Reference peak}}} \quad (1)$$


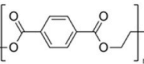
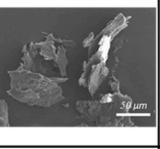

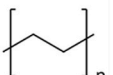
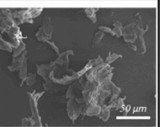

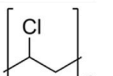
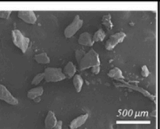

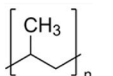
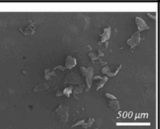

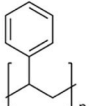
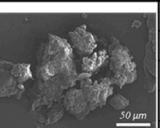
where $A_{\text{Carbonyl group}}$ is the maximum absorbance height of the carbonyl group; $A_{\text{Reference peak}}$ is the maximum absorbance height of the reference peak for each MP.

After testing different peaks as reference, those that did not present any significant difference along the Fenton process were selected (1017, 722, 612, 1376, 1493 cm^{−1} for PET, PE, PVC, PP, EPS, respectively).

2.3. Fenton oxidation of micro- and nanoplastics

Oxidation experiments (7.5 h) of MPs and NPs were performed at 80 °C and acidic pH (pH₀ = 3) in a glass batch reactor (75 mL) under constant stirring (200 rpm). These relatively severe operating conditions were selected after conducting preliminary experiments under ambient conditions where no significant changes were found in the MPs along the oxidation process (data not shown). In the experiments devoted to the oxidation of MPs, the initial MP mass was set at 100 mg, while the initial concentrations of Fe³⁺ and H₂O₂ were established at 10 mg L^{−1} and 1000 mg L^{−1}, respectively. On the other hand, in the oxidation of NPs, the initial concentration of the plastic particles was set at 20 mg L^{−1} (1.5 mg in 75 mL), while the initial concentrations of Fe³⁺ and H₂O₂ were established at 10 mg L^{−1} and 130 mg L^{−1}, respectively. To enhance the oxidation yield, additional doses of Fe³⁺ (1 mL, 750 mg L^{−1}) were added to the reactor every 1.5 h. In the case of H₂O₂, additional doses (1 mL, 75 g L^{−1} for MPs oxidation; 1 mL, 9.75 g L^{−1} for NPs oxidation) were added to the reactor every 0.5 h (once complete consumption of H₂O₂ was reached). A final experiment was carried out to evaluate the degradation of leachates with diethyl-phthalate (DEP) as target pollutant under similar operating conditions ([DEP]₀ = 5 mg L^{−1},

Table 1
Main characteristics of the MPs studied in this work.

	Raw material	Molecular structure	SEM image	Mean particle size (µm)	Elemental analysis (CHNS) (% wt.)	CI	Water contact angle (°)	pH _{slurry}
PET	 Disposable water bottle			157.0	C: 62.4; H: 5.1; N: <0.1; S: <0.1 O ^a : 32.5	1.31	118.5 ± 3.6	8.7
PE	 Micropipette tips			170.0	C: 84.8; H: 14.4; N: <0.1; S: <0.1 O ^a : 0.8	0.05	122.7 ± 2.8	8.7
PVC	 Pipeline			201.0	C: 37.5; H: 6.3; N: 0.3; S: 0.1 Cl ^b : 55.8	0.03	118.3 ± 3.7	9.1
PP	 Disposable vials			198.0	C: 83.8; H: 14.1; N: 0.2; S: <0.1 O ^a : 1.8	0.03	124.0 ± 2.0	8.8
EPS	 Food tray			27.0	C: 91.3; H: 8.0; N: 0.1; S: <0.1 O ^a : 0.6	0.09	118.3 ± 1.8	8.7
				54.5		0.08	120.0 ± 0.5	8.9
				101.0		0.10	117.3 ± 3.5	9.0
				187.0		0.09	118.0 ± 1.3	8.9
				335.0		0.10	119.8 ± 0.8	8.8

^a Calculated by difference.

^b Determined in deionized water at pH₀ = 6.

[Fe³⁺]₀ = 10 mg L⁻¹, [H₂O₂]₀ = 20.65 mg L⁻¹, 80 °C, pH₀ = 3). Iron was fed as Fe³⁺ instead of Fe²⁺ leading to a Fenton-like process of similar characteristics as the conventional one (Pignatello et al. (2006)). Blank experiments carried out at the same operating conditions but in the absence of Fe³⁺ and H₂O₂ allowed to discard any influence of the temperature and acidity on the changes suffered by the MPs along the oxidation process. Likewise, experiments carried out with H₂O₂ but in the absence of catalyst led to negligible changes in the solids, allowing to confirm that Fenton oxidation was the responsible for the changes observed in the oxidation of MPs/NPs in this work.

The MPs degradation yield achieved upon Fenton experiments was determined by measuring the loss of weight. For such goal, MPs residues after the oxidation experiments were collected by filtration through a pre-weighed 0.45 µm PTFE filter, then air dried (60 °C) and weighed as the solid product. MPs were not washed before the analyses except for optical microscopic analyses where a subtle acid washing (HNO₃, 0.1 M) of the oxidized MPs was performed to remove iron residues from the surface of the plastic particles to better appreciate any morphological change. To follow the oxidation yield along the experiment carried out with PS NPs, total organic carbon (TOC) was measured. It must be noted that the suspension of PS NPs in water was fairly stable, so TOC measurements offered a reliable approach to determine their concentration and thus, the extension of the reaction. Samples were periodically taken from the reactor and immediately analysed. A TOC analyser (Shimadzu, mod. TOC VSCH) was used. H₂O₂ concentration was determined by colorimetric titration following the titanium sulphate method (Eisenberg (1943)).

2.4. Biodegradability of MPs leachates

The leaching of both fresh and oxidized MPs was analysed in terms of biodegradability following the procedure described elsewhere (Romer-a-Castillo et al. (2018)). Firstly, MPs leaching experiments were carried out incubating under artificial solar radiation (HQI-T Powerstar lamp, UV-A radiation by 2 Philips TL100 W/10 R fluorescent tubes and UV-B radiation by 2 UVA-340 fluorescent lamps) and in a water bath at 28 °C, simulating the surface waters in some areas of the coastal Mediterranean Sea in summer. EPS MPs in the range from 100 to 250 µm (fresh and oxidized) at a concentration of 9 g L⁻¹ were added to 250 mL of sterilized (autoclaved at 121 °C for 20 min) artificial seawater (36.9 g L⁻¹ using Sea Salt from Sigma-Aldrich) in quartz tubes which were incubated for 6 days of exposure time. After incubation period, samples for dissolved TOC were collected after filtration through a combusted GF/F filter (Whatman). Afterwards, the bioavailability of the dissolved TOC leached from plastics was evaluated. An inoculum of 0.8 µm filtered surface seawater from the Blanes Bay Microbial Observatory, in the coastal NW Mediterranean Sea, was added to the leaching solutions at a ratio of 9:1 (leachate: inoculum). Then, NH₄Cl (10 µmol L⁻¹) and NaH₂PO₄ (2 µmol L⁻¹) were added to avoid microorganisms growth limitation by either nitrogen or phosphorus availability. The flasks were incubated in the dark at 23 °C until the mixed microbial community reached the stationary phase. All the experiments were carried out in triplicate. Dissolved TOC samples were collected at the beginning and at the end of the exponential phase (4 days). Samples for microbial abundance were collected daily.

Bacterial abundance was measured by flow cytometry (BD FACS-Calibur) following the method described elsewhere (Gasol and Del Giorgio (2000)).

3. Results and discussion

3.1. Microplastics characterization

The characterization of the MPs studied in this work is collected in Table 1. As can be appreciated in the SEM images, also included in Table 1 (see Fig. S1 of the Supplementary Material for optical

microscopic images), the MPs obtained after cryogenic milling were essentially irregular and rough-shape fragments. With respect to particle size, the results were consistent with the sieving, obtaining in all cases a mean particle size within the corresponding sieving size-range. The elemental analysis (CHNS) and the FTIR analysis (see Figs. S2-S10 of the Supplementary Material for FTIR spectra) were in good agreement with the corresponding polymer of the raw materials, which allowed to confirm a high degree of purity of the raw plastic products. On the other hand, these results also proved that after the grinding process, the polymer did not present any change in its composition with respect to the starting material. The CI values calculated from FTIR spectra were very similar for PE, PVC, PP and EPS, but a significantly higher value was found for PET. This is clearly due to the chemical structure of the polymers. PET was the only polymer that contain carbonyl groups in its structure (Table 1). On the other hand, the variation in the size of EPS MPs did not lead to any change in the CI estimation, so it can be confirmed that the chemical structure of EPS did not change with decreasing the particle size.

To characterize the hydrophobicity/hydrophilicity of each MP, water contact angle measurements were carried out. As can be seen in Table 1, values within the range of 118–124° were obtained for all the materials studied, clearly above 90°, typical of hydrophobic solids (Yuan and Lee (2013)). Specifically, the highest water contact angle values were obtained for PE (122.7°) and PP (124.0°). The higher hydrophobicity of these solids was also visually evident as they were less susceptible to being properly wetted. On the other hand, it must be noted that the different EPS MP sizes did not show noticeable changes in the water contact angle values, which confirms the high reproducibility of the measurement technique regardless of the particle size.

To get further insights on the surface chemical composition of the MPs, the pH_{slurry} of the MPs was also determined. The results obtained operating at pH₀ = 6 are collected in Table 1 (see Table S1 of the Supplementary Material for complete experimental data obtained at different initial pH values). In accordance with their hydrophobic nature, basic pH_{slurry} values within the range of 8–9 were obtained, confirming the basic character of all the MPs regardless their nature or size.

3.2. Fenton oxidation of microplastics

To evaluate the extension of the oxidation reaction, the MPs weight loss was measured at the end of the experiments and the properties of the solids were fully characterized. As can be seen in Fig. 1a, somewhat low weight losses were found considering the relatively severe operating conditions tested. Weight loss values were close to 10% regardless of the nature of the MP, which demonstrates the high stability of these solids towards hydroxyl radicals attack. Considering the dose of H₂O₂ employed and the loss of weight achieved, the extrapolated amount of H₂O₂ to completely remove (weight loss) a unit mass of MPs was around 107 g_{H2O2} g_{MP}⁻¹ oxidized (equivalent to 116 g_{H2O2} g_{TOC}⁻¹ mineralized). This value is remarkably higher than the previously reported for the treatment of industrial wastewaters under similar operating conditions (Pliego et al. (2012); Munoz et al. (2014); Munoz et al. (2016)), where values between 10 and 20 g_{H2O2} g_{TOC}⁻¹ mineralized were obtained, which further demonstrates the extremely high persistence of MPs. Apart from considering the impact of the MPs nature on their overall degradation, the influence of the particle size was also investigated. For such goal, EPS MPs of five different particle size ranges between 20 and 500 µm were evaluated (Fig. 1b). Although low weight losses were also found, they clearly followed a trend with the MP particle size. The weight loss value achieved after the oxidation process visibly increased with decreasing the MP particle size. While a weight loss value around 10% was achieved in the Fenton oxidation of 250–500 µm MP, almost 20% was reached when 20–50 µm MP were treated. Consistent with these results, the amount of H₂O₂ needed to completely remove (weight loss) a unit mass of MPs was substantially decreased with decreasing the size of the MPs (values of 113, 107, 94, and 63 g_{H2O2} g_{MP}⁻¹ oxidized, equivalent to

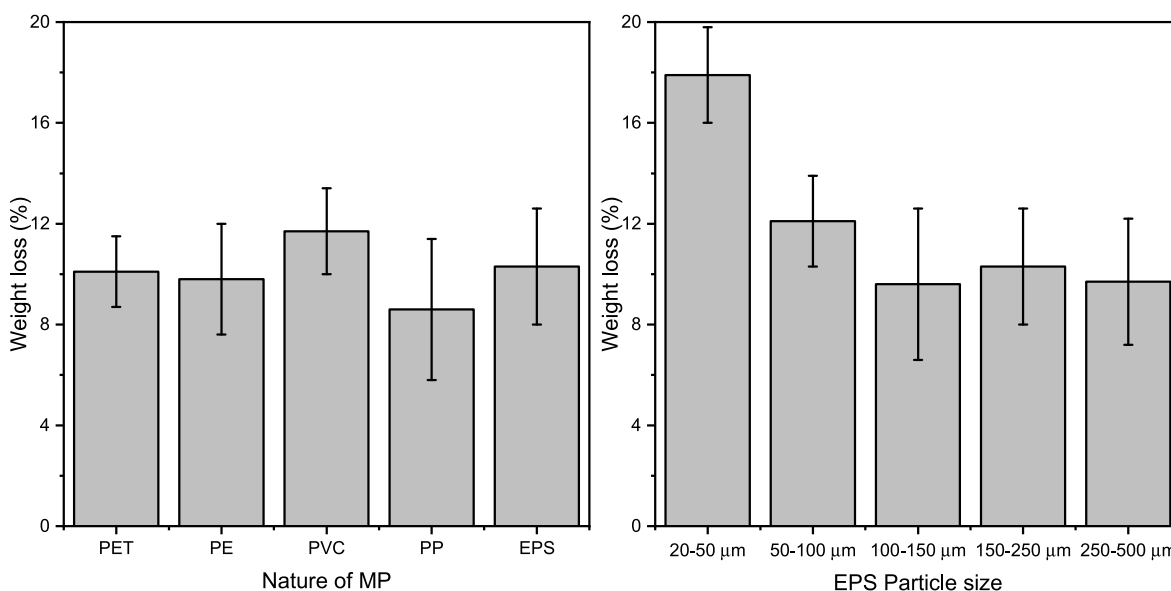


Fig. 1. Influence of nature of MP (a) and EPS particle size (b) on the weight loss of the MPs after Fenton treatment.

123, 116, 102 and 69 $\text{g}_{\text{H}_2\text{O}_2} \text{g}_{\text{TOC}}^{-1}$ mineralized, were obtained for the oxidation of 250–500, 150–250, 50–100 and 20–50 µm MP, respectively). Since smaller microparticles have a larger exposed surface area, these results seem to indicate that the reaction takes place on the MP surface, which is attacked by hydroxyl radicals. Once the surface of the solid is completely degraded, new parts of the MP are exposed, thus presumably continuing the reaction.

As previously indicated in the introduction, the Fenton process has been proposed in the literature as a pre-treatment for the isolation of MPs in real aqueous matrices for analytical purposes since other organic solids are expected to be oxidized to a higher extent given the persistence of plastics (Lares et al. (2018); Tagg et al. (2016); Hurley et al. (2018)). However, although our results corroborate that subtle degradation of MPs occurs regardless of their nature, they also prove that the

use of the Fenton process as a pre-treatment for MPs quantification may lead to an underestimation of the undersized MPs present in the starting sample as they are clearly degraded to a greater extent. Accordingly, the operating conditions of the Fenton process must be carefully optimized to warrant that MPs remain unchanged along the oxidation treatment for MPs isolation purposes.

Despite the relatively low MPs weight losses achieved after Fenton oxidation, the particles suffered important changes on their surface along reaction. As representative example, Fig. 2 shows images of the EPS MPs suspensions in deionized water before and after the oxidation treatment, together with light microscopic and SEM images (light microscopic and SEM microscopic images of all of the MPs tested in this work, both fresh and oxidized, are collected in Fig. S1; S11–S13 of the Supplementary Material). As can be observed, while fresh EPS MPs float

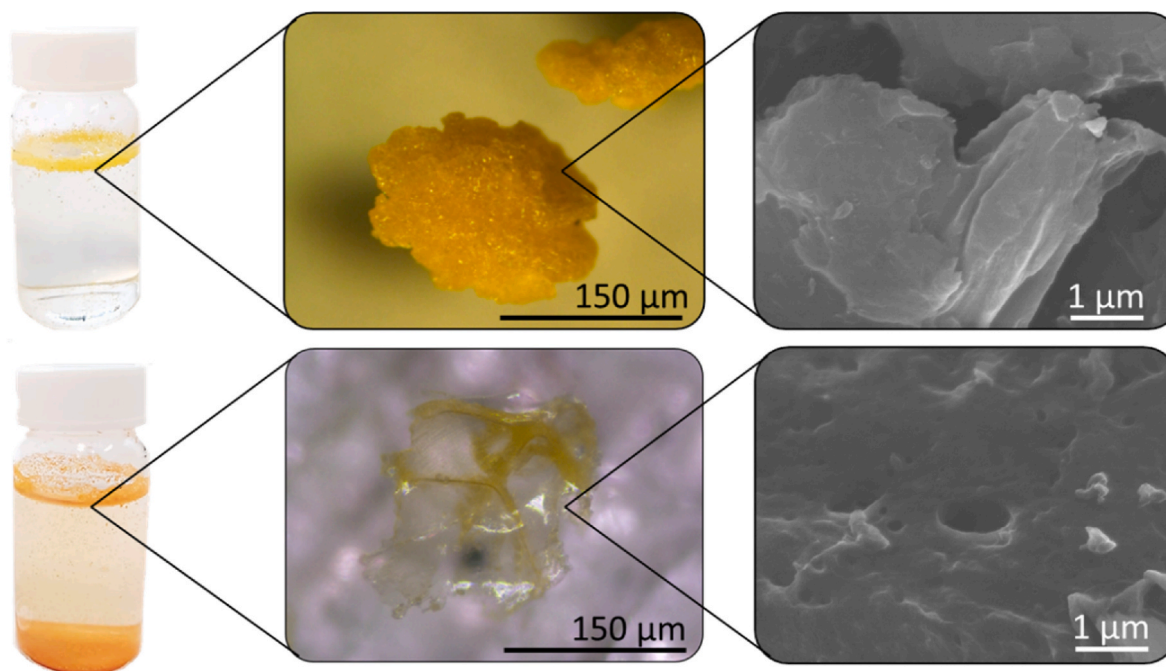


Fig. 2. Fresh EPS suspension (a), fresh EPS light microscopic image (b), fresh EPS SEM image (c), oxidized EPS suspension (d), oxidized EPS light microscopic image (e) and oxidized EPS SEM image (f).

on the water matrix, a clear indication of their high hydrophobicity, the oxidized ones were distributed throughout the liquid and even settled. This visual observation suggests that after the Fenton treatment MPs become more hydrophilic, thus allowing better contact with the water phase. On the other hand, by comparing the optical microscopy images, it can be seen that oxidized MPs showed semi-transparent areas not observed in the fresh solids. This fact confirms that the reaction starts at the surface of the particles, progressively degrading them and causing a decrease in their thickness. Finally, SEM images revealed the presence of wrinkles, voids, and holes on the MP surface, which could not be observed in the fresh particles.

All these modifications were especially evident in PET and EPS MPs, probably due to their molecular structure. The presence of aromatic rings in these MPs may increase the oxidation yield by generating differences in electronic charge along the polymer structure. In fact, it is well known that hydroxyl radicals preferentially attack aromatic rings and double bonds compared with alkanes (Pignatello et al. (2006)). These results are in good agreement with those reported by Lang et al. (2020), who recently studied the ageing of EPS MPs (~600 µm) by the Fenton process. After 7 days of reaction ($[H_2O_2]_0 = 4500 \text{ mg L}^{-1}$; $[Fe^{2+}]_0 = 167.5 \text{ mg L}^{-1}$; room temperature and $pH_0 = 4$), the MPs showed a rougher surface, with small cracks and holes. Furthermore, a growth in the adsorption capacity of Cd^{2+} was observed upon oxidation of the MP, suggesting that surface modifications have occurred. In fact, an increase of surface oxygenated groups was detected, and new absorption bands in the infrared spectrum (corresponding to the C–O, C=O, and O–C=O bonds) were observed.

To further investigate the surface changes observed in the different MPs after the Fenton process, the main properties of the oxidized materials were characterized. The water angle contact, CI, pH_{slurry} and mean particle size of the oxidized MPs are listed in Table 2. Comparing the contact angle results, a clear decrease in this parameter was obtained after the Fenton oxidation treatment, which corroborates the increase in the hydrophilicity of the MPs. Regarding the MP nature, the variation in the water angle contact value was particularly noticeable in the case of PET and EPS. In fact, the water droplet spread completely on the MPs layer in these cases leading to a nearly zero apparent contact angle for PET and most of EPS MP sizes. Therefore, these oxidized MPs could be classified as superhydrophilic solids, since they could not be accurately measured by the optical system employed ($<5\text{--}10^\circ$) (Drelich and Chibowski (2010)). Only the smallest EPS MPs tested ($<50 \text{ µm}$) could be measured, probably due to the smoother and more homogeneous surface of the obtained MP layer compared to that of higher MP sizes, where more irregularities are present favouring the fast penetration of the water droplet. In any case, the water contact angle value was reduced around 70% also in this case, confirming that the oxidation process is clearly increasing the hydrophilicity of the MPs (see Fig. S14 of the Supplementary Material for water angle contact measurements with fresh and oxidized EPS MPs ($<50 \text{ µm}$)). In contrast to the results obtained with PET and EPS, the MPs composed by alkane polymers i.e. PE, PVC and PP showed slight changes in their water contact angle values

after oxidation ($<6\%$ reduction) (Table 2). Again, these results can be explained by the significantly lower reactivity of alkane polymers towards hydroxyl radicals attack compared to aromatic rings-bearing polymers (Lares et al. (2018)). On the other hand, the observed percentage reductions in the water contact angle values for the alkane-bearing polymers were 6%, 5% and $<2\%$ for PE, PP and PVC MPs, respectively, which indicates that the presence and nature of substituents also affects the oxidation yield. PE does not present any substituent, which seemed to favour its hydrophilization compared to the substituted alkanes. PP, which contains methyl substituents, showed a slightly lower hydrophilization than PE due to the presence of such electro-neutral groups; whereas PVC, which contains chlorine substituents, was the least hydrophilized MP probably due to the protection offered by the halogen towards hydroxyl radical attack. In fact, it is well known that $HO\cdot$ does not readily attack halogens and favours the least substituted carbons due to its electrophilic character (Pignatello et al. (2006)).

The surface oxidation after the Fenton treatment led to a significant reduction of the pH_{slurry} from basic (8–9) to slightly acidic values (4–5) for all MPs (Table 2). These results are consistent with the aforementioned changes in the water contact angle values after treatment, since the surface hydrophilicity is clearly related to the presence of oxygenated groups which acidify the solid surface (Shi et al. (2009)). According to the results obtained for the oxidation of different particle sizes of EPS MPs, the pH_{slurry} of the MP decreased with decreasing its particle size, which is consistent with the higher exposed surface of the solid (Table 2). The oxidation process degrades the microparticles progressively from the surface of the material, thus decreasing the particle size and increasing the exposed surface area, leading to a higher degradation rate of the solids.

The decrease in water contact angle and pH_{slurry} indicates that oxygenated groups are incorporated on the surface of the solids through the Fenton oxidation reaction (Liu et al. (2019)). Upon Fenton process, different polar functional groups may be generated like hydroxyl, carbonyl, carboxyl, alcohol, ketone, peroxy and ester groups, which promotes the previously observed increase in the hydrophilicity of the surface. To check the possible generation of oxygenated groups, the CI was calculated from FTIR spectra for each oxidized sample (Table 2). It must be noted that despite the subtle changes in the carbonyl peak position ($1850\text{--}1650 \text{ cm}^{-1}$), the FTIR spectra of all MPs remained practically unchanged after Fenton oxidation (see Figs. S2–S10 of the Supplementary Material for FTIR spectra of both fresh and oxidized MPs). On the other hand, it must be noted that no significant changes were found in the elemental analyses of oxidized microplastics compared with the fresh ones, and thus, it can be concluded that the chemical composition of these solids remained unchanged after Fenton treatment. Comparing the CI of the oxidized solids with the fresh ones, a clear increase can be seen in all MPs samples except PVC. An increase in the CI is consistent with the incorporation of carboxylic groups on the surface of the solids after the oxidation process. The increase of CI was higher for those MPs with aromatic groups in their chemical structure (PET and EPS), while a more subtle rise in CI was found for the rest of the MPs studied (alkane-based polymers). A special case is PVC, where the increase of this parameter is practically negligible. This result is consistent with the lower hydrophilization observed for this plastic and again, can be related to the protection offered by the chlorine substituent of the alkane chain towards hydroxyl radical attack (Pignatello et al. (2006)). On the other hand, it is important to note that the MP size also showed an impact on the generation of carboxyl groups. Clearly, higher CI values were obtained with decreasing the EPS MP size. While the oxidation of the smallest EPS MP size ($<50 \text{ µm}$) led to an increase of the CI from 0.09 to 0.24, only 0.14 was achieved with the highest EPS MP size range tested (250–500 µm). These results corroborated that small particles with a larger exposed surface area favours the incorporation of oxygenated groups and thus, the oxidation of the MP. Liu et al. (2019) obtained similar results when they compared the aging of PS and

Table 2
Main surface properties of oxidized MPs.

MP	Mean particle size (µm)	CI	Water contact angle (°)	pH_{slurry}
PET	123.0	1.42	^a	5.4
PE	163.0	0.10	115.5 ± 3.2	4.5
PVC	193.0	0.04	116.3 ± 3.3	4.2
PP	192.0	0.10	118.0 ± 2.5	4.6
EPS	24.1	0.24	36.0 ± 4.8	4.7
	48.9	0.21	^a	4.9
	88.3	0.20	^a	5.2
	169.0	0.18	^a	5.1
	300.0	0.14	^a	5.4

^a Not measurable. The drop of water was quickly adsorbed by the layer of MPs, confirming its high hydrophilicity.

PE MPs the Fenton process. After 30 days of reaction ($[\text{H}_2\text{O}_2]_0 = 4500 \text{ mg L}^{-1}$; $[\text{Fe}^{2+}]_0 = 167.5 \text{ mg L}^{-1}$; ambient temperature and $\text{pH}_0 = 4$), an increase of nearly 0.15 and 0.05 in CI estimation was obtained for PS and PE, respectively.

The MPs hydrophilization due to the incorporation of oxygenated groups on their surface have serious implications on the behaviour of the MPs. For instance, it is well-known that MPs can act as pollutant carriers in the aquatic environment given their high exposed surface areas (Magni et al. (2019); Ma et al. (2019); Bhat and Gogate (2021); Serrano et al. (2020)). The hydrophilization of the MPs could completely change the adsorption performance of MPs. In fact, in our previous contribution (Munoz et al. (2021)), where the role of MPs on the adsorption of micropollutants was investigated, we found that the Fenton oxidation of MPs led to a significant decrease on their adsorption capacity of a hydrophobic micropollutant, the anti-inflammatory diclofenac, while substantially increased the uptake of a hydrophilic pharmaceutical, the antibiotic metronidazole.

Apart from considering the surface modification of the MPs upon Fenton oxidation, the impact of this treatment on their size was also evaluated (Table 2). MPs suffered a slight decrease in their particle size after reaction being this effect especially noticeable for PET (~20%) and EPS (~11%), the polymers with aromatic rings in their structures. More discrete changes (~3%) were observed for the alkane polymers i.e. PE, PVC and PP. These results are in good agreement with the main findings observed in the surface modification of MPs, where clearly those polymers containing aromatic rings were more susceptible to Fenton oxidation than those based on alkane chains. Surprisingly, these data differ from the obtained by Liu et al. (2019), who observed a clear decrease in mean particle size in both cases, but this decrease was notably larger for PE than for PS. The main reason behind this rather unexpected result can be attributed to the different tensile strength of the fresh MPs tested. In the current work, expanded EPS was tested in contrast to the conventional and clearly more dense PS employed in the study of Liu et al. (2019). In fact, these authors mentioned that PS was more prone to chemical attack than PE, which resulted in a faster oxidation of PS in the initial time. However, the higher tensile strength of the PS (56.2 MPa) employed as target material compared to that of PE (27.6 MPa) led to a greater size decrease in the latter plastic. It must be noted that the tensile strength of the EPS foam used as target material in this study is rather low (<1 MPa) (Gnip et al. (2007); Chen et al. (2015)) and thus, it did not offer the same resistance of conventional PS towards

fragmentation. On the other hand, the initial size of the MP tested did not show a relevant impact on the particle reduction yield, which indicates that this phenomenon is obviously much slower than the hydrophilization of the MPs surface.

To get deeper insights onto the reduction of MPs particle size along Fenton oxidation, particle size distributions were also analysed. As representative example, Fig. 3 shows the particle size distribution of EPS MPs (150–250 μm) before and after Fenton oxidation (see Figs. S15–S23 of the Supplementary Material for the experimental data obtained with all the MPs tested). Clearly, oxidized MPs showed a lower proportion of large particles (>200 μm) than the fresh MPs, while the opposite trend was observed for the smaller particles (<200 μm). These results are consistent with the above-mentioned hypothesis, evidencing that MPs are progressively breaking down along the oxidation process. The effect of the oxidation by Fenton process, and other related AOPs, on the size of MPs has been scarcely investigated in the literature, probably due to the high persistency of these solids (Jiang et al. (2021); Liu et al. (2019)). Evidently, size reduction is only observed when the oxidation of MPs is remarkably high, i.e. their surface has been strongly oxidized and oxygen functional groups are largely introduced. All in all, these results are in agreement with the work of Liu et al. (2019), where a progressive increase in the proportion of smaller microparticles of PE and PS throughout the Fenton oxidation was found while studying the aging behaviour of MPs.

Although all the experiments performed were carried out using deionized water as reaction matrix, no significant changes are expected neither in the extension nor in the rate of the process if waters with a low content of organic matter and/or inorganic ions would be treated considering the relatively severe operating conditions in terms of temperature (80 °C) but also in terms of H_2O_2 dose (10 g L^{-1}) employed in this work.

3.3. Fenton oxidation of nanoplastics

In the previous section, it was demonstrated that the oxidation of MPs is started on the surface of the solids leading to the formation of oxygen functional groups, which consequently increase their acidity and hydrophilicity and progressively reduce their size, ultimately resulting in subtle weight losses. Assuming that MPs would continue their size reduction along Fenton oxidation and to get deeper insights onto the extension of the oxidation process and thus the mineralization yield, a

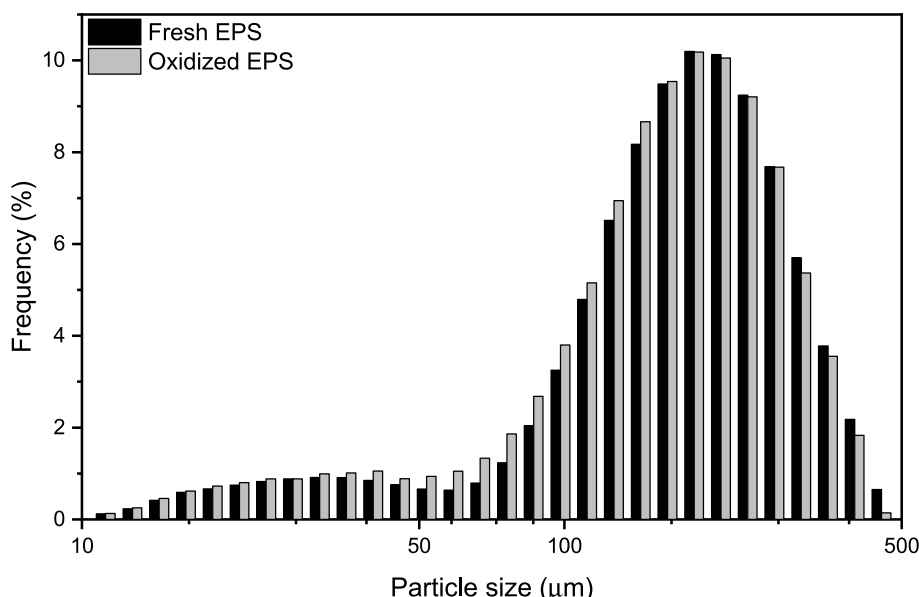


Fig. 3. Particle size distribution of EPS 150–250 μm .

new experiment was carried out using commercial PS NPs (140 nm). As these particles were homogeneously dispersed in water and did not settle, the evolution of their concentration was followed by analysing the TOC along reaction. Evidently, not only the solid particles but also possible organic leachates released from the NPs to the liquid phase would be considered, that is why the evolution of the reaction was also followed by periodically analysing the solid particles by TEM microscopy.

Fig. 4 collects the TEM images of the solid particles at each reaction stage together with the evolution of TOC along Fenton oxidation of PS NPs. As can be seen, fresh PS NPs were smooth spheres with a completely homogeneous particle size. Along Fenton oxidation, they suffered important changes and particle breakdown, leading in the end to an undefined agglomerated solid composed by NPs fragments. Consistent with these observations, TOC concentration was progressively decreased along reaction, reaching up to 70% mineralization after applying 15 doses of H_2O_2 . Considering the dose of H_2O_2 employed and the degree of mineralization achieved, the amount of H_2O_2 needed to completely mineralize a unit mass of NPs was $21.5 \text{ g}_{\text{H}_2\text{O}_2} \text{ g}_{\text{NP(ToC)}}^{-1}$. This value is quite close to those previously reported in the literature for the treatment of real wastewaters (Pliego et al. (2012); Munoz et al. (2014); Munoz et al. (2016)). For instance, in our previous contributions (Munoz et al. (2014); Munoz et al. (2016)), values of 12.1 and $14.3 \text{ g}_{\text{H}_2\text{O}_2} \text{ g}_{\text{TOC}}^{-1}$ mineralized were required in the treatment of sawmill and hospital wastewaters, respectively. These results clearly demonstrate that hydroxyl radical attack can completely mineralize the plastic particles and opens the door for the intensification of the process so it could be applied for water treatment purposes, which was out of the scope of the current study.

Since the release of organic leachates along the oxidation of MPs/NPs is expected, an additional experiment focused on the degradation of a dissolved plasticizer was also carried out to determine if the presence of dissolved species in the water phase can substantially affect the kinetics and extension of MPs/NPs oxidation, or if these compounds would even remain in the liquid phase once the solid particles are removed. For such goal, diethyl phthalate (DEP), one of the most frequently used plasticisers in numerous plastic materials was selected (Cao et al. (2022)). This experiment was performed under similar operating conditions to those previously used for the oxidation of MPs and NPs (the main properties of the phthalate and the oxidation stoichiometry are provided in Table S2 of the Supplementary Material). Notably, the

complete degradation of DEP was achieved after 2 h reaction time using the stoichiometric H_2O_2 dose for its complete degradation (H_2O_2 and Fe^{3+} were added only at the beginning of the reaction, see Fig. S24 of the Supplementary Material for experimental results). These results highlight the high degradation rate of these compounds compared to the degradation of MPs and NPs. Therefore, it can be concluded that the possible leachates produced during the process will be also degraded in the course of the reaction.

The obtained results imply that, on the one hand, the size of the solid is a critical factor when using this technology for the oxidation of MPs and NPs. Clearly, NPs are more prone to be oxidized by Fenton oxidation given their higher exposed surface. On the other hand, it is demonstrated that plastic residues can be finally mineralized, including the possible leachates released from the solids.

3.4. Biodegradability of oxidized MPs leachates

It is well-known that along AOP treatments, the intermediates generated can show even more harmful than the target compounds (da Silva et al. (2014); Munoz et al. (2011); de Luna et al. (2014)) and thus, the study of the biodegradability of the leachates released from the solids to the aqueous phase offers a deeper understanding of the Fenton oxidation of MPs/NPs and its potential environmental implications. Once demonstrated that MPs underwent a surface chemical oxidation that ultimately resulted in high mineralization yields, the possible leaching of MPs upon Fenton reaction was analysed in terms of biodegradability following the procedure described elsewhere (Romera-Castillo et al., 2018). For this study, EPS MPs (100–250 μm) were selected. After six days of incubation (photodegradation in aqueous saline media), simulating the surface seawaters, fresh and oxidized EPS microplastics leached 104 and 205 μM of dissolved TOC, respectively. Bacterial incubation assays were carried out afterwards using those leaching solutions. Remarkably, 24 and 63 μM of dissolved TOC were consumed in the fresh and oxidized EPS microplastics, respectively, which are in the same range than other commercial plastics under similar conditions (Romera-Castillo et al., 2022). In fact, bacterial abundance was higher in the solution coming from the oxidized EPS sample compared to the fresh one, resulting in $5.4 \cdot 10^{-6}$ and $3.5 \cdot 10^{-6}$ cell mL^{-1} at the end of the biodegradation experiments, respectively. Therefore, it was confirmed that the leachates from oxidized EPS MPs did not inhibit bacterial growth, and in fact, they were even more

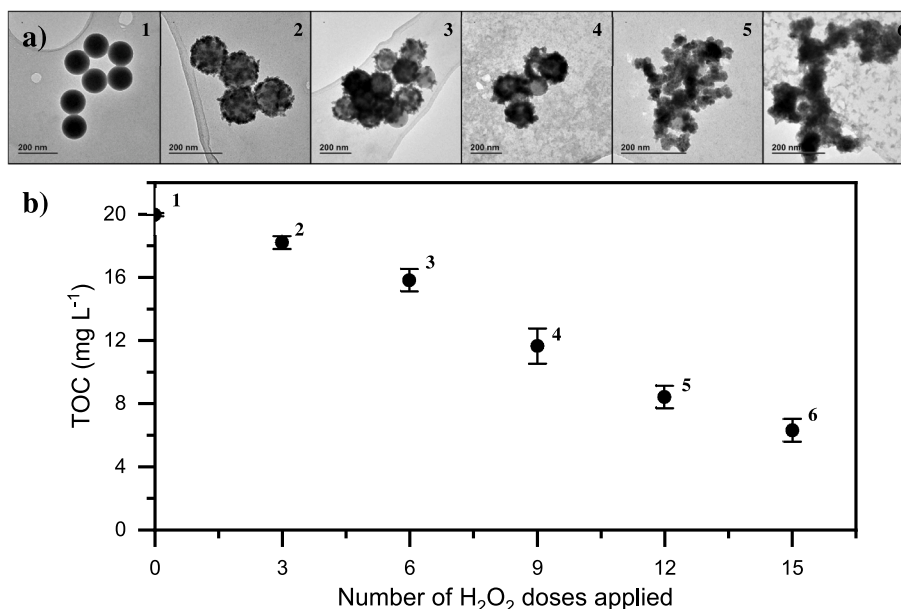


Fig. 4. Degradation of PS NPs along the oxidation reaction. TEM images (a), TOC (b).

biodegradable than the leachates released from the fresh solids since 30% and 23% of the dissolved TOC was consumed, respectively.

4. Conclusions

The results obtained in this work have demonstrated that MPs undergo important changes along intensified Fenton treatment. The oxidation process starts in the particle surface, leading to its physical/morphological modification (creation of wrinkles, voids, and holes) and also chemical alteration due the formation of oxygen functional groups, which consequently increase its hydrophilicity and surface acidity. Furthermore, MPs progressively reduce their size, which ultimately results in their complete oxidation to CO₂. The nature of the plastic particles has a relevant impact on its overall oxidation, being more prone to be oxidized those polymers which contain aromatic rings in their structures (EPS and PET) compared to those formed by aliphatic chains (PE, PP and PVC). In the latter, the presence of substituents as chlorine increases their resistance to be oxidized. Clearly, the decrease of MPs particle size increases their reactivity achieving high oxidation yields due to the higher exposed surface area readily available to be attacked by hydroxyl radicals. Along the oxidation process, which occurs from the surface to the core of plastic particles, the release of leachates is assumed. Nevertheless, these dissolved species are remarkably more quickly oxidized than the solid particles. Notably, dissolved oxidation intermediates do not inhibit bacterial growth, and in fact, they can be even more biodegradable than the leachates released from the fresh solids. All this knowledge is crucial for the understanding of the fate of MPs along Fenton oxidation and opens the door for the design and optimization of this process for water treatment. Furthermore, it offers relevant information that must be considered when the application of Fenton is intended for MPs analytical purposes as the oxidation can significantly modify the solid particles and even remove those of smaller ranges, leading to an underestimation in the quantification of MPs.

Author contributions statement

Conceptualization: Macarena Munoz, David Ortiz; Funding acquisition: Macarena Munoz, Zahara M. de Pedro, Jose A. Casas; Investigation: David Ortiz, Julia Nieto-Sandoval, Cristina Romera-Castillo; Methodology: David Ortiz, Zahara M. de Pedro; Project administration: Jose A. Casas; Supervision: Macarena Munoz, Jose A. Casas; Roles/Writing - original draft: David Ortiz, Macarena Munoz; Writing - review & editing: Zahara M. de Pedro, Jose A. Casas.

Declaration of competing interest

The authors declare that they have no known competing financial interests or personal relationships that could have appeared to influence the work reported in this paper.

Data availability

Data will be made available on request.

Acknowledgments

This research has been supported by the Autonoma University of Madrid and Community of Madrid through the project SI1-PJI-2019-00006, and by the Spanish MINECO through the project PID2019-105079RB-I00. D. Ortiz thanks the Spanish MIU for the FPU predoctoral grant (FPU19/04816). M. Munoz and J. Nieto-Sandoval thank the Spanish MINECO for the Ramón y Cajal postdoctoral contract (RYC-2016-20648) and the FPI predoctoral grant (BES-2017-081346), respectively. C. Romera-Castillo was supported by JIN-2019 project (PID2019-109889RJ-I00) from the Spanish Ministry of Science and Innovation and the Agencia Estatal de Investigación and acknowledges

the “Severo Ochoa Centre of Excellence” accreditation (CEX2019-000928-S).

Appendix A. Supplementary data

Supplementary data to this article can be found online at <https://doi.org/10.1016/j.chemosphere.2022.136809>.

References

- Ariza-Tarazona, M.C., Villarreal-Chiu, J.F., Hernández-López, J.M., De la Rosa, J.R., Barbieri, V., Siligardi, C., Cedillo-González, E.I., 2020. Microplastic pollution reduction by a carbon and nitrogen-doped TiO₂: effect of pH and temperature in the photocatalytic degradation process. *J. Hazard Mater.* 395, 122632.
- Bhat, A.P., Gogate, P.R., 2021. Degradation of nitrogen-containing hazardous compounds using advanced oxidation processes: a review on aliphatic and aromatic amines, dyes, and pesticides. *J. Hazard Mater.* 403, 123657.
- Cao, Y., Lin, H., Zhang, K., Xu, S., Yan, M., Leung, K.M.Y., Lam, P.K.S., 2022. Microplastics: a major source of phthalate esters in aquatic environments. *J. Hazard Mater.* 432, 128731.
- Chen, W., Hao, H., Hughes, D., Shi, Y., Cui, J., Li, Z., 2015. Static and dynamic mechanical properties of expanded polystyrene. *Mater. Eng.* 69, 170–180.
- Cox, K.D., Covernton, G.A., Davies, H.L., Dower, J.F., Juanes, F., Dudas, S.E., 2019. Human consumption of microplastics. *Environ. Sci. Technol.* 53 (12), 7068.
- da Silva, J.C., Reis Teodoro, J.A., Afonso, R.J., Aquino, S.F., Augusti, R., 2014. Photodegradation of bisphenol A in aqueous medium: monitoring and identification of by-products by liquid chromatography coupled to high-resolution mass spectrometry. *Rapid Commun. Mass Spectrom.* 28 (9), 987–994.
- de Luna, L.A.V., da Silva, T.H.G., Nogueira, R.F.P., Kummrow, F., Umbuzeiro, G.A., 2014. Aquatic toxicity of dyes before and after photo-Fenton treatment. *J. Hazard Mater.* 276, 332–338.
- Drelich, J., Chibowski, E., 2010. Superhydrophilic and superwetting surfaces: definition and mechanisms of control. *Langmuir* 26 (24), 18621–18623.
- Ebrahimbabaie, P., Yousefi, K., Pichtel, J., 2022. Photocatalytic and biological technologies for elimination of microplastics in water: current status. *Sci. Total Environ.* 806, 150603.
- Eisenberg, G., 1943. Colorimetric determination of hydrogen peroxide. *Industrial and engineering chemistry. Anal. Ed.* 15 (5), 327–328.
- Enfrin, M., Lee, J., Gibert, Y., Basheer, F., Kong, L., Dumée, L.F., 2020. Release of hazardous nanoplastic contaminants due to microplastics fragmentation under shear stress forces. *J. Hazard Mater.* 384.
- Gasol, J.M., Del Giorgio, P.A., 2000. Using flow cytometry for counting natural planktonic bacteria and understanding the structure of planktonic bacterial communities. *Sci. Mar.* 64 (2), 197–224.
- Gnip, I.Y., Vejeliš, S., Kersulis, V., Vaitkus, S., 2007. Deformability and tensile strength of expanded polystyrene under short-term loading. *Polym. Test.* 26 (7), 886–895.
- Hurley, R.R., Lusher, A.L., Olsen, M., Nizzetto, L., 2018. Validation of a method for extracting microplastics from complex, organic-rich, environmental matrices. *Environ. Sci. Technol.* 52, 7409–7417.
- Jiang, R., Lu, G., Yan, Z., Liu, J., Wu, D., Wang, Y., 2021. Microplastic degradation by hydroxy-rich bismuth oxychloride. *J. Hazard Mater.* 405, 124247.
- Lang, M., Yu, X., Liu, J., Xia, T., Wang, T., Jia, H., Guo, X., 2020. Fenton aging significantly affects the heavy metal adsorption capacity of polystyrene microplastics. *Sci. Total Environ.* 722, 137762.
- Lares, M., Ncibi, M.C., Sillanpää, M., Sillanpää, M., 2018. Occurrence, identification and removal of microplastic particles and fibers in conventional activated sludge process and advanced MBR technology. *Water Res.* 133, 236–246.
- Li, J., Liu, H., Paul Chen, J., 2018. Microplastics in freshwater systems: a review on occurrence, environmental effects, and methods for microplastics detection. *Water Res.* 137, 362–374.
- Liu, P., Qian, L., Wang, H., Zhan, X., Lu, K., Gu, C., Gao, S., 2019. New insights into the aging behavior of microplastics accelerated by advanced oxidation processes. *Environ. Sci. Technol.* 53 (7), 3579–3588.
- Ma, B., Xue, W., Ding, Y., Hu, C., Liu, H., Qu, J., 2019. Removal characteristics of microplastics by Fe-based coagulants during drinking water treatment. *J. Environ. Sci.* 78, 267–275.
- MacArthur, D.E., Waughray, D., Stuchtey, R.M., 2016. The New Plastics Economy: Rethinking the Future of Plastics. *World Economic Forum*.
- Magni, S., Binelli, A., Pittura, L., Avio, C.G., Della Torre, C., Parenti, C.C., Gorbi, S., Regoli, F., 2019. The fate of microplastics in an Italian wastewater treatment plant. *Sci. Total Environ.* 652, 602–610.
- Mason, S.A., Garneau, D., Sutton, R., Chu, Y., Ehmann, K., Barnes, J., Fink, P., Papazissimos, D., Rogers, D.L., 2016. Microplastic pollution is widely detected in US municipal wastewater treatment plant effluent. *Environ. Pollut.* 218, 1045–1054, 1987.
- Miranda, M.N., Sampaio, M.J., Tavares, P.B., Silva, A.M.T., Pereira, M.F.R., 2021. Aging assessment of microplastics (LDPE, PET and uPVC) under urban environment stressors. *Sci. Total Environ.* 796, 148914.
- Munoz, M., de Pedro, Z.M., Casas, J.A., Rodríguez, J.J., 2011. Assessment of the generation of chlorinated byproducts upon Fenton-like oxidation of chlorophenols at different conditions. *J. Hazard Mater.* 190 (1), 993–1000.

- Munoz, M., Pliego, G., de Pedro, Z.M., Casas, J.A., Rodriguez, J.J., 2014. Application of intensified Fenton oxidation to the treatment of sawmill wastewater. *Chemosphere* 109, 34–41.
- Munoz, M., Garcia-Muñoz, P., Pliego, G., de Pedro, Z.M., Zazo, J.A., Casas, J.A., Rodriguez, J.J., 2016. Application of intensified Fenton oxidation to the treatment of hospital wastewater: kinetics, ecotoxicity and disinfection. *J. Environ. Chem. Eng.* 4, 4107–4112.
- Munoz, M., Ortiz, D., Nieto-Sandoval, J., de Pedro, Z.M., Casas, J.A., 2021. Adsorption of micropollutants onto realistic microplastics: role of microplastic nature, size, age, and NOM fouling. *Chemosphere* 283, 131085.
- Nabi, I., Bacha, A., Ahmad, F., Zhang, L., 2021. Application of titanium dioxide for the photocatalytic degradation of macro- and micro-plastics: a review. *J. Environ. Chem. Eng.* 9 (5), 105964.
- Pignatello, J.J., Oliveros, E., MacKay, A., 2006. Advanced oxidation processes for organic contaminant destruction based on the Fenton reaction and related chemistry. *Crit. Rev. Environ. Sci. Technol.* 36 (1), 1–84.
- Plastics Europe, 2021. **Plastics-the Facts 2021 an Analysis of European Plastics Production, Demand and Waste Data.** <https://plasticseurope.org/knowledge-hub/plastics-the-facts-2021/>.
- Pliego, G., Zazo, J.A., Blasco, S., Casas, J.A., Rodriguez, J.J., 2012. Treatment of highly polluted hazardous industrial wastewaters by combined coagulation-adsorption and high-temperature Fenton oxidation. *Ind. Eng. Chem. Res.* 51, 2888–2896.
- Rezania, S., Park, J., Md Din, M.F., Mat Taib, S., Talaiekhazani, A., Kumar Yadav, K., Kamyab, H., 2018. Microplastics pollution in different aquatic environments and biota: a review of recent studies. *Mar. Pollut. Bull.* 133, 191–208.
- Romera-Castillo, C., Pinto, M., Langer, T.M., Álvarez-Salgado, X.A., Herndl, G.J., 2018. Dissolved organic carbon leaching from plastics stimulates microbial activity in the ocean. *Nat. Commun.* 9, 1430.
- Romera-Castillo, C., Mallenco-Fornies, R., Saá-Yáñez, M., Álvarez-Salgado, X.A., 2022. Leaching and bioavailability of dissolved organic matter from petrol-based and biodegradable plastics. *Mar. Environ. Res.* 176, 105607.
- Serrano, E., Munoz, M., de Pedro, Z.M., Casas, J.A., 2020. Fast oxidation of the neonicotinoid pesticides listed in the EU Decision 2018/840 from aqueous solutions. *Separ. Purif. Technol.* 235, 116168.
- Shi, K., Kokini, J.L., Huang, Q., 2009. Engineering zein films with controlled surface morphology and hydrophilicity. *J. Agric. Food Chem.* 57 (6), 2186–2192.
- Sol, D., Laca, A., Laca, A., Díaz, M., 2020. Approaching the environmental problem of microplastics: importance of WWTP treatments. *Sci. Total Environ.* 740, 140016.
- Tagg, A.S., Harrison, J.P., Ju-Nam, Y., Sapp, M., Bradley, E.L., Sinclair, C.J., Ojeda, J.J., 2016. Fenton's reagent for the rapid and efficient isolation of microplastics from wastewater. *Chem. Commun.* 53 (2), 372–375.
- Wu, C., Zhang, K., Huang, X., Liu, J., 2016. Sorption of pharmaceuticals and personal care products to polyethylene debris. *Environ. Sci. Pollut. Control Ser.* 23 (9), 8819–8826.
- Yang, T., Luo, J., Nowack, B., 2021. Characterization of nanoplastics, fibrils, and microplastics released during washing and abrasion of polyester textiles. *Environ. Sci. Technol.* 55 (23), 15873.
- Yuan, Y., Lee, T.R., 2013. *Contact Angle and Wetting Properties. Surface Science Techniques.* Springer Berlin, Heidelberg, pp. 3–34.